Research article

Preparation and optimization of niosome encapsulated meropenem for significant antibacterial and anti-biofilm activity against methicillin-resistant *Staphylococcus aureus* isolates

Kamal Paseban [a], Sama Noroozi [b], Rokhshad Gharehcheloo [c], Abbas Haddadian [d], Farnoush Falahi Robattorki [e], Hedieh Dibah [f], Reza Amani [g], Fatima Sabouri [h], Erfan Ghanbarzadeh [i], Shadi Hajrasouiha [f], Arezou Azari [f], Tina Rashidian [j], Amir Mirzaie [j,*], Zahra Pirdolat [f], Massoumeh Salarkia [f], Dorsa Sadat Shahrava [f], Fatemeh Safaeinikjoo [f], Atena Seifi [f], Niusha Sadat Hosseini [k], Niloofar Saeinia [k], Aliasghar Bagheri Kashtali [f,**], Ali Ahmadiyan [f], Roza Mazid Abadi [f], Faezeh Sadat Kermani [f], Romina Andalibi [f], Arman Chitgarzadeh [f], Aryan Aryan Tavana [f], Tohid Piri Gharaghie [f]

[a] *Department of Biology, Zanjan Branch, Islamic Azad University, Zanjan, Iran*
[b] *Department of Neurology, University of Utah, Utah, USA*
[c] *Department of Pharmacology, Pharmaceutical Branch, Islamic Azad Universty, Tehran, Iran*
[d] *Department of Biology, East Tehran Branch, Islamic Azad University, Tehran, Iran*
[e] *Biomedical Engineering Group, Chemical Engineering Department, Engineering Faculty, Tarbiat Modares University, Tehran, Iran*
[f] *Department of Biology, Roudehen Branch, Islamic Azad University, Roudehen, Iran*
[g] *Biotechnology Research Center, Shahrekord Branch, Islamic Azad University, Shahrekord, Iran*
[h] *International Acedemy of Georgia, Georgia*
[i] *Department of Microbiology, Faculty of Medicine, Guilan University of Medical Sciences, Rasht, Iran*
[j] *Department of Biology, Parand Branch, Islamic Azad University, Parand, Iran*
[k] *Department of Biology, Science and Research Branch, Islamic Azad University, Tehran, Iran*

ARTICLE INFO

ABSTRACT

Background: One of the targeted drug delivery systems is the use of nanocarriers, and one of these drug delivery systems is niosome. Niosome have a nano-vesicular structure and are composed of non-ionic surfactants. Objective: In this study, various niosome-encapsulated meropenem formulations were prepared. Subsequently, their antibacterial and anti-biofilm activities were evaluated against methicillin-resistant *Staphylococcus aureus* (MRSA) strains.

Methods: The physicochemical properties of niosomal formulations were characterized using a field scanning electron microscope, X-Ray diffraction, Zeta potential, and dynamic light scattering. Antibacterial and anti-biofilm activities were evaluated using broth microdilution and minimum biofilm inhibitory concentration, respectively. In addition, biofilm gene expression analysis was performed using quantitative Real-Time PCR. To evaluate biocompatibility, the

* Corresponding author.
** Corresponding author.
E-mail addresses: Amir_mirzaie92@yahoo.com (A. Mirzaie), Bagheri-ali@riau.ac.ir (A. Bagheri Kashtali).

cytotoxicity of niosome-encapsulated meropenem in a normal human diploid fibroblast (HDF) cell line was investigated using an MTT assay.

Results: An F1 formulation of niosome-encapsulated meropenem with a size of 51.3 ± 5.84 nm and an encapsulation efficiency of 84.86 ± 3.14 % was achieved. The synthesized niosomes prevented biofilm capacity with a biofilm growth inhibition index of 69 % and significantly downregulated *icaD, FnbA, Ebps*, and *Bap* gene expression in MRSA strains ($p < 0.05$). In addition, the F1 formulation increased antibacterial activity by 4–6 times compared with free meropenem. Interestingly, the F1 formulation of niosome-encapsulated meropenem indicated cell viability >90 % at all tested concentrations against normal HDF cells. The results of the present study indicate that niosome-encapsulated meropenem increased antibacterial and anti-biofilm activities without profound cytotoxicity in normal human cells, which could prove useful as a good drug delivery system.

1. Introduction

Methicillin-resistant *Staphylococcus aureus* (MRSA) is a type of bacterium that causes infections in humans. MRSA strains are among the most common pathogens in hospitals and a leading cause of hospital-acquired illnesses. In addition, MRSA strains cause dangerous and purulent infections and death in hospitalized patients [1]. These strains are known to be the leading prevalent pathogens of hospital-acquired infections and are resistant to a wide variety of antibiotics, such as methicillin [2]. The use of efficient antibiotics began in the 1960s because of the high mortality rate associated with MRSA strains [3]. Meropenem and vancomycin are two of the most commonly used antibiotics for the treatment of infections caused by MRSA [4]. Meropenem is a broad-spectrum antibiotic used to treat bacterial illnesses, such as pneumonia, meningitis, sepsis, and anthrax [5]. Meropenem is typically administered as a preventative medicine for individuals with systemic infections [6]. Meropenem, when combined with other antibiotics, boosts its effectiveness against MRSA strains, according to an earlier study [7]. Meropenem overuse has increased the number of enterococci harboring the meropenem resistance gene during the last decade. As a result, plasmids encoding resistance genes have a high chance of conjugating with *S. aureus* strains [8]. Since 1996, MRSA strains have been identified, and they pose a significant threat to healthcare systems [9]. Another explanation for antibiotic resistance in MRSA strains is biofilm development, which has become a major concern in the field of hospital-acquired infections. Biofilms are cohesive microbial communities enclosed in an extracellular polymer matrix that form on animate or inanimate surfaces [10]. Biofilms can cause many complications if they form on oil reservoirs, air conditioning systems, and medical equipment such as prostheses and catheters. In addition, biofilms increase antibiotic resistance [11]. Several genes, including *icaD, FnbA, Ebps*, and Bap fibronectin binding genes, are involved in biofilm formation in MRSA strains [12–17]. Researchers have been using nanomaterials to generate more and more newer drug delivery systems as a result of the emergence of antibiotic resistance and the slow pace of developing new antibiotics in recent years. Low-cost production and no environmental issues are among the advantages that have turned nanoparticles into one of the most suitable drug-delivery systems for drug delivery to target areas [18–20]. Niosomes have recently been identified as a drug-delivery system for antimicrobial agents that improves selective drug delivery and antimicrobial drug therapeutic efficacy. Niosomes are bilayer structures whose nonionic surfactants make them water-soluble and enable them to carry high drug doses [21,22]. Recent studies have focused on the use of niosome as drug delivery systems for antimicrobial agents [23]. In this study, a niosome-encapsulated meropenem was selected to inhibit MRSA and enhance its antimicrobial effects. To achieve this objective, meropenem was employed as a model antimicrobial agent, and MRSA strains were selected as test organisms. Finally, the antimicrobial anti-biofilm effects of meropenem-containing niosomes against MRSA strains were investigated and compared with those of free meropenem.

2. Experimental section

2.1. Methods

2.1.1. Preparation of niosomes encapsulated meropenem

According to the instructions provided by previous studies, the niosome encapsulation of meropenem was conducted through thin-

Table 1
Primers used in this study.

Gene	Primer sequence (5′ to 3′)
icaD	F ATGGTCAAGCCCAGACAGAG
	R CGTGTTTTCAACATTTAATGCAA
FnbA	F CGCTGATGTTGTTGAATATGAAGAAGATAC
	R TGTTGTATGATCGCTCACTG
Ebps	F CATCCAGAACCAATCGAAGAC
	R CTTAACAGTTACATCATCATGTTTATCTTTG
Bap	F CCCTATATCGAAGGTGTAGAATTGCAC
	R GCTGTTGAAGTTAATACTGTACCTGC

film hydration and 4 drug compounds were prepared as follows (25, 26). The first compound contained Span 60 (CAS: 1338-41-6) (Henan Daken Chemical CO., LTD., China) and Tween 60 (CAS: 9005-67-8) (career Henan chemical co, China) mixed with cholesterol (CAS: 57-88-5) (Capot Chemical Co., Ltd., China) at respective molar ratios of 3:3:4 and was dissolved in 10 ml of chloroform and methanol mixed at respective ratios of 2:1. The second compound contained Span 40 (CAS: 26,266-57-9) (Henan Daken Chemical CO., LTD., China) and Tween 40 (CAS: 9005-66-7) (Shanghai Jizhi Biochemical Technology Co., Ltd, China) mixed with cholesterol (CAS: 57-88-5) (Capot Chemical Co., Ltd., China) at respective molar ratios of 3:3:4 and was dissolved in 10 mL of chloroform and methanol mixed with respective ratios of 2:1. The third compound contained Span 60 and Tween 40 mixed with cholesterol at respective molar ratios of 3:3:4 and was dissolved in 3 ml of chloroform and methanol mixed at respective ratios of 2:1. The fourth compound was made up of Span 40 and Tween 60 combined with cholesterol in 3:3:4 molar ratios and dissolved in 3 ml chloroform and methanol combined in 2:1 molar ratios (Table 1) After adding glass beads to all four compounds, the drug compound solvents were evaporated using a rotary evaporator (Heidolph, Germany) for 1 h at 60 °C and 120 rpm rotation. The dried thin films were hydrated for 1 h using a solution of meropenem (1 mg/mL) dissolved in 10 mL of PBS at 60 °C and 120 rpm to obtain different niosome formulations. The resulting particles were sonicated using a probe sonicator in an ice bath with SONOPULS ultrasonic homogenizers (amplitude: 25 %, 200 wt) for 5 min to reduce the size of the niosomes containing meropenem, and samples were stored at 4 °C until the next experiments.

2.2. Characterization of prepared niosomes

The average size, size distribution, and zeta potential of the niosome-encapsulated meropenem were obtained using dynamic light scattering (DLS) and Zeta-plas-palladium electrodes (Brookhaven Instruments Corp., USA). Various newly prepared niosome formulations were diluted two times using distilled water at a ratio of 20:1 to prevent multiple scattering as a result of interactions between particles, and analysis was conducted at 25 °C with a 90° light scattering angle. The average z diameter and niosome multiple scattering index were determined, and their zeta potentials were measured. Niosome-encapsulated meropenem particles were coated with a gold layer to generate electrical conductivity and were examined using a field scanning electron microscope (FESEM) device model MIRA3 (TESCAN, Czech Republic) and an XRD device model X 'Pert Pro (Panalytical, Netherlands). The peak relative intensities provide insight into the atomic distribution in the unit cell, whereas the XRD patterns provide information about the particle size and flaws. A good peak-to-background ratio is critical for proper powder diffractogram interpretation. Background information in powder diffraction can be obtained from various sources, including the apparatus and sample. The crystalline phase of the adsorbent is determined by analyzing the XRD patterns and diffraction peaks.

2.3. Entrapment efficiency (EE)

The encapsulation efficiency was determined by determining the amount of non-capsule meropenem (free meropenem) in the formed niosome. Niosome-encapsulated meropenem particles were isolated for over an hour at 4 °C in a refrigerated centrifuge at 1400 rpm. The meropenem content of the supernatant was examined through an ELISA Reader Stat Fax2100's (Awareness Technology, Ukraine) light absorbance reading of the supernatant at a wavelength of 276 nm, and the EE percentage was calculated based on equation (1):

$$\%EE = ((\text{Drug added} - \text{Free "unentrapped drug"})/\text{Drug added}) \times 100 \tag{1}$$

2.4. In-vitro drug release study and stability

Dialysis was performed to examine meropenem release of the niosome. The dialysis tube was soaked in distilled water for 24 h. Then, 0.5 ml (10 mg) of meropenem-loaded noodles was placed in the dialysis bag, and 0.5 ml of meropenem antibiotic aqueous solution containing 10 mg of meropenem was used as a control sample. Dialysis bags were immersed in conical flasks containing 75 ml of distilled water and shaken at 50 rpm in a water bath at 37 °C. Five milliliters were withdrawn from the receptor medium at intervals of one, two, four, six, 12, and 24 h, and meropenem was measured in terms of spectrophotometry at 281 nm. Aliquots of samples were replaced with a new medium at 37 °C, and diffusion profiles were determined using various kinetic models. This method was used to monitor the stability of various niosome-encapsulated meropenem formulations at 7, 14, 21, 28, 35, 42, 49, and 56 days for a storage period of two months at 25 °C.

2.5. Clinical samples and Staphylococcus aureus isolation

In total, 300 clinical samples from the Shariati (100 samples), Firoozgar (100 samples), and Rasoul Akram (100 samples) hospitals in Tehran were collected. *S. aureus* strains were collected from clinical samples including blood, wound, urine, and cerebrospinal fluid. Samples were cultivated in blood agar cultures using sterile swabs at 37 °C for 24 h. *S. aureus* isolates were identified using microbiological tests, including Gram staining, catalase, mannitol fermentation, and DNase. Finally, the molecular identification of bacteria was performed using 16S rDNA and PCR.

2.6. Antibiotic sensitivity test

The antibiotic susceptibility of *S. aureus* to various antibiotics was examined by disk diffusion according to the Clinical and Laboratory Standards Institute (CLSI) method after *S. aureus* strains were detected and confirmed. *The sensitivity of S. aureus isolates to* vancomycin (VA, 10 µg), cefoxitin (FOX, 10 µg), ciprofloxacin (CIP, 5 µg), clindamycin (CD, 2 µg), mupirocin (MU, 5 µg), and meropenem (MEM, 10 µg) (MAST, UK) disks was measured in Muller–Hinton agar culture (Merck, Germany). Cefoxitin antibiotic discs were used to identify methicillin-resistant *Staphylococcus aureus* (MRSA) strains. *The Staphylococcus aureus* ATCC 33592 standard strain was used as the positive control, whereas the negative control was *Staphylococcus epidermidis* ATCC 14990. Screening for resistance to vancomycin was performed according to the method proposed by Tiwary et al. (2006, 24) in a Brain Heart Infusion (BHI) culture containing 6 mg of vancomycin (BHI6V) per liter.

2.7. Biofilm formation assay

A microtiter plate assay was used to determine the ability of the isolates to form biofilms. Through this assay, isolates were incubated at 37 °C for 24 h after cultivation in a TSB (Tryptic soy broth) culture medium containing 0.5 % glucose. After emptying the wells and washing with phosphate-buffered saline solution (PBS), staining was performed using 1 % violet crystals. The adhered cells were suspended in 33 % glacial acetic acid (Merck, Germany). Ethanol (70 %) was added to each well, and the light absorbance was examined using an ELISA Reader Stat Fax2100 (Awareness Technology, Ukraine) at a wavelength of 570 nm. Biofilm formation results were reported in four classifications: non-binding (OD ≤ 0.083), weak (ODC < OD ≤ 2 × ODC), moderate (2 × ODC < OD ≤ 4 × ODC), and strong (OD > 4 × ODC) [23].

2.8. Molecular detection of biofilm-related genes

Genomic DNA of the bacteria was obtained using the instructions of the CinnaGene extraction kit (Cinna Pure DNA KIT, Alborz, Iran), and its purity at 260 nm was confirmed using a spectrophotometer. Multiplex PCR was conducted to detect biofilm-encoding genes, including *icaD, FnbA, Ebps, and Bap, using the* oligonucleotide sequences of specific primers (Table 1). The final reaction volume (20 µL) was considered to contain 12 µL PCR master mix (PCR buffer, MgCl2, dNTP, 0.2 units of Taq polymerase), 0.5 µL reverse primer, 0.5 µL forward primer, 1 µL template cDNA, and 6 µL distilled water (Amplicon, Denmark). The PCR program was performed in the form of an initial denaturation at 95 °C for 5 min and 35 initial denaturation cycles of 1 min at 94 °C, 1 min of connection at 58 °C, 1 min of extension at 72 °C, and a final extension at 72 °C for 5 min. The amplified products were investigated using 1 % agarose gel electrophoresis to detect the desired genes.

2.9. Antibacterial activity

The antibacterial activity of various niosome-encapsulated meropenem formulations against MRSA was examined using broth microdilution. The minimum inhibitory concentration (MIC) and minimum bactericidal concentration (MBC) were then determined as follows. After culturing MRSA strains in Müller-Hinton broth for 24 h, the 5×10^5 CFU/mL of bacteria, 100 µl of various niosome-encapsulated meropenem formulations, free meropenem, and free niosome (in a concentration ranging from 0.03 to 64 µg/ml), and 95 µl Muller Hinton broth were poured into each well of a 96-well plate and incubated for 24 h at 37 °C. The MIC and MBC were determined. In addition, negative control (containing pure culture medium) and positive control (containing culture medium plus the standard *Staphylococcus aureus* strain ATCC 33592) were used, and this test was performed in triplicate [24].

2.10. Anti-biofilm activity of niosome-encapsulated meropenem

The ½ MIC concentrations of free meropenem and various formulations of niosome-encapsulated meropenem were used to determine the minimum biofilm inhibition concentration (MBIC) against the MRSA strains constituting the mature biofilm. The wells of a 96-well plate were filled with 100 µl drug samples and 100 µl of bacteria cultured in Müller Hinton Broth (5×10^5 CFU/mL). The plates were incubated for 48 h at 37 °C and were stained with crystal violet after washing. The tests were replicated twice, and the mean MBIC was determined to be OD630 < 0.1. This test was performed in triplicate [25,26].

2.11. Inhibition of biofilm growth

According to Vyas et al. [27], the effectiveness of niosome-encapsulated meropenem in inhibiting biofilm growth through adhesion to model biofilms was determined by measuring the reduction in OD630 of biofilms exposed to free and niosome-encapsulated meropenem for 2 h. Biofilm-containing wells were treated with 200 µl niosome-encapsulated meropenem at various concentrations (0.5, 0.75, 1, 1.5, and 2 times the MIC). Free meropenem and meropenem mixed with blank niosomes were used as control samples. After 2 h of incubation at 37 °C, the liquid contents of each well were aspirated, and the biofilms were washed with ethanol. Afterward, an antibiotic-free culture was added to the wells, and the liquid contents of the biofilm and aspirate were fixed and washed. Biofilms were stained using violet crystals, and their light absorbance was measured using an ELISA Reader Stat Fax2100 (Awareness Technology, Ukraine) at 630 λ_{max} nm wavelength, and the biofilm growth inhibition (%BGI) was calculated using equation (2):

$$BGI\% = \{''[OD630 \times UntreatedBiofilm] - [OD630 \times TreatedBiofilm]'' \div (OD630 \times UntreatedBiofilm)\} \times 100 \qquad \text{(Equation 2)}$$

2.12. Biofilm gene expression analysis

The expression of the biofilm genes icaD, *FnbA*, *Ebps*, and *Bap* were examined using quantitative polymerase chain reaction (qRT-PCR) with specific primers (16). RNA was extracted from MRSA strains using an RNX-Plus kit (Sina gene, Iran) after 24 h of being exposed to ½ MIC concentrations of free meropenem and niosome-encapsulated meropenem, and cDNA was synthesized based on the RNA extracted from treated and untreated strains according to the protocol of the YTA Kit (Yekta Tajhiz, Iran). The final reaction volume was 15 μl, containing 1 μl of cDNA, 1 μl of the forward primer and 1 μl of the reverse primer, 8 μl of master mix, and 4 of μl deionized water (Merck, Germany). The temperature cycle included initial denaturation for 5 min at 95 °C followed by 40 cycles of 20 s at 95 °C, 40 s at 58 °C, and 40 s at 72 °C. The final stage was selected to be at 53–95 °C to draw melting curves [28].

2.13. Cytotoxicity

The in vitro cytotoxicity of niosome-loaded meropenem, free meropenem, and free meropenem in human diploid fibroblasts (HDF normal cells) was investigated using ((3- (Method 4, 5-dimethylthiazole-2-yl) −2) 5- Diphenyl-tetrazolium bromide (MTT) assay. For this purpose, after seeding 10×10^4 cells onto a 96-well microtiter plate at 37 °C in an atmosphere of 5 % CO_2, treated with different concentrations of niosome-loaded meropenem, and incubated for 24 h at 37 °C. Subsequently, 100 μl MTT dye (5 mg/ml) were poured into the wells, and incubation was continued at 37 °C for 4 h. The supernatant was then removed followed by adding 100 μl DMSO and shaking for 5 min. The absorbance of each well was estimated using a microplate reader (AccuReader, Metrotech, Taiwan) at 570 nm. Eventually, cell viability was calculated using equation (3) [24,29,30]:

$$\text{Cell viability } \% = (\text{OD570 sample / OD570 control}) \times 100 \qquad \text{(Equation 3)}$$

2.14. Statistical analysis

The data were expressed as SD, and statistical analysis was performed using GraphPad Prism (version 5.01) and a one-way ANOVA test used for statistical analysis. $p < 0.05$ was considered significant.

3. Results

3.1. Formulation of niosomes and their characterization

Various formulations of niosome-encapsulated meropenem were prepared in terms of various indicators, such as the surfactant-to-cholesterol ratio, Span-to-Tween ratio, and the composition of different surfactants (Table 2). Each formulation exhibited a distinct size, polydispersity index (PDI), and entrapment efficiency (EE%). Dynamic Light Scattering (DLS) analysis revealed that various formulations of niosome-encapsulated meropenem exhibited good uniformity (Table 3). As demonstrated, F1 is of a smaller and better size and is associated with the surfactant Span 60 hydrophile-lipophile balance. Span 60 had a hydrophile-lipophile balance of 4.7, whereas the corresponding value for Span 40 was 6.7. Therefore, the nanoparticles developed with Span 60 are smaller. In addition, the EE% of the F1 formulation was higher than that of the other formulations, which might be due to the surfactant used. A longer saturated alkyl chain is directly associated with drug permeability in niosomes; thus, longer saturated alkyl chains enhance drug permeability. Span 60 has a longer alkyl chain than Span40, which is why formulations incorporating Span 60 have higher indexes and EE% is at its peak in F1. Polydispersity indexes (PDI) smaller than 0.3 indicate a suitable distribution of small nanoparticles, indicating

Table 2
Different formulations of niosomal meropenem.

Formulations	Different compounds of surfactant: Cholesterol	Span + Tween + Cholesterol molar ratio	Span: Tween molar ratio	Drug concentration (mg/ml)
F1	Span 60+ Tween 60+ Cholesterol	3:3:4	50:50	1
			25:75	1
			75:25	1
F2	Span 40+ Tween 40+ Cholesterol	3:3:4	50:50	1
			25:75	1
			75:25	1
F3	Span 60+ Tween 40+ Cholesterol	3:3:4	50:50	1
			25:75	1
			75:25	1
F4	Span 40+ Tween 60+ Cholesterol	3:3:4	50:50	1
			25:75	1
			75:25	1

that the F1 formulation is optimal given its smallest PDI. As shown in Fig. 1A, SEM results indicated a uniform spherical shape in the niosome-encapsulated meropenem of the F1 formulation with an average size of 51.3 nm, indicating a suitable diameter (<100) of this drug formulation (Fig. 1A). Also, other formulations (F2–F4) (Fig. 1B, C and 1D) and free niosomes had a spherical structure (Fig. 1E and F). As the diagram resulting from X-ray diffraction indicates (Fig. 2), the presence of niosomes was confirmed in the 2θ range at 20–80°. The four diffraction peaks observed in the XRD spectrum of the sample at angles higher than 37° were associated with reflections (111), (200), (220), and (311) at 38.141°, 46.251°, 64.49°, and 77.57°, confirming the presence of meropenem in the niosome particles. A comparison of peak intensities reveals that peak 111 is more intense than the other three.

Morphologic features of niosome-encapsulated meropenem, such as average size and encapsulation efficiency (EE), were examined to evaluate its stability at various temperatures and time intervals. Results indicated that increasing temperature changed the morphological features of niosome-encapsulated meropenem and increased its size, resulting in decreased EE%, whereas increasing the shelf life did not have any significant effects on its EE% and morphological features (Fig. 3). According to the results, various drug formulations exhibited higher stability at 4 °C than at 25 °C, indicating the negative impact of temperature on the stability of encapsulated drugs. On the other hand, the F1 niosome-encapsulated meropenem formulation was the most stable among the other formulations.

3.2. In vitro drug release

The amount of meropenem released from the niosome was examined using the dialysis bag method. Meropenem release from niosomes exhibited a two-phase release pattern consisting of blast and stable phases; the stable constant peaked after 7 h in various formulations. The released amount of antibiotic then started declining and the release speed increased with a gentle slope for up to 72 h. Lower drug release speeds in the blast phase were associated with higher encapsulation efficiency and more effective controlled drug release. Therefore, the highest efficiencies of controlled emission were attributed to formulations F1, F3, F4, and F2, with respective release percentages of 45, 48, 52, and 56 in the blast phase. The F1 formulation had the highest efficiency in controlled diffusion, showing a 98.2 ± 1.6 % drug release after 312 h, whereas free meropenem release was 89 ± 2.41 % in the blast phase, which increased to 99 ± 1.1 % in 72 h (Fig. S1).

3.3. Isolation, antibiotic susceptibility test, and biofilm formation test

Out of the 300 collected clinical samples, 162 *S. aureus* isolates were identified using microbial diagnostic tests, and further molecular examination by 16S rDNA PCR confirmed the identification of *S. aureus* strains (data not shown). Subsequently, the sensitivity of *S. aureus* isolates to various antibiotics was studied which indicated that out of the 162 isolates, 60 isolates (37 %) were multidrug-resistant (MDR), whereas 40 (24.69 %) were methicillin-resistant *S. aureus* (MRSA). In addition, 23 samples (57.5 %) of 40 MDR isolates formed biofilms. Among the biofilm-forming MRSA strains, only 6 strains (SMRSA1, SMRSA2, SMRSA3, SMRSA4, SMRSA5, and SMRSA6) were vancomycin-resistant. Of the examined bacterial strains, six and the *S. aureus* ATCC 33592 isolate were biofilm-generating. To investigate the presence of biofilm genes, including *Bap, icaD, FnbA,* and *Ebps*, multiplex PCR was performed using specific primers. The results showed that vancomycin-resistant MRSA strains had all genes simultaneously (Fig. S2, Table 4).

3.4. Antibacterial activity

To examine the antibacterial activity of niosome-encapsulated meropenem and free meropenem, the minimum inhibitory concentration (MIC) and minimum bactericidal concentration (MBC) were determined against MRSA strains. The various formulations of niosome-encapsulated meropenem and free meropenem were treated against 6 MRSA *S. aureus* (that were MDR and vancomycin resistance), including SMRSA1, SMRSA2, SMRSA3, SMRSA4, SMRSA5, and SMRSA6, as well as *S. aureus* ATCC 33592. The results demonstrated that among the various formulations, F1 decreased the MIC value approximately 4–6 times compared with free meropenem (Table 5).

3.5. Anti-biofilm activity

The ability of niosomes carrying meropenem to inhibit the growth of MRSA isolates through adhesion to biofilms over a short period following exposure to drug formulations was compared with that of free meropenem. Compared with the minimum biofilm inhibitory concentration (MBIC) study, the biofilm growth inhibition condition was harder since the biofilm was first treated for only 2

Table 3
Characteristics of the niosome-encapsulated meropenem compared with the free niosome.

Formulations	Polydispersity index (average ± SD)	Zeta Potential (m.v)	Vesicle size (nm) (SEM(	EE (%)
Free niosome	0.314 ± 0.99	−75.12 ± 1.75	0.615.42 ± 0.84	–
F1	0.131 ± 0.014	−65.29 ± 2.68	51.3 ± 5.84	84.86 ± 3.14
F2	0.272 ± 0.025	−68.75 ± 2.84	218.1 ± 14.26	63.28 ± 1.83
F3	0.163 ± 0.004	−67.85 ± 2.12	96.8 ± 7.21	76.08 ± 0.23
F4	0.192 ± 0.016	−68.15 ± 1.75	176.7 ± 9.19	71.26 ± 3.24
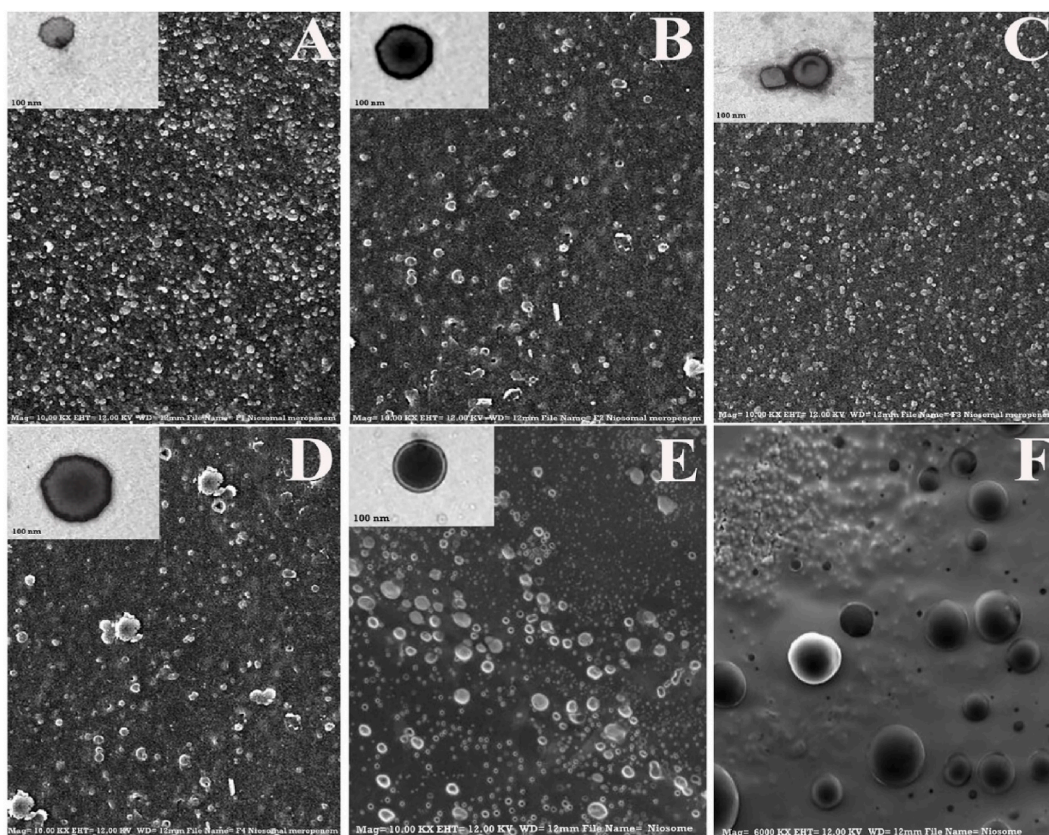
Fig. 1. A) FESEM of F1 formulation B) FESEM of F2 formulation C) FESEM of F3 formulation D) FESEM of F4 formulation, E, F) FESEM of free niosome.

h with drug formulations or free meropenem; biofilms were then washed and incubated in an antibiotic-free medium for 24 h. This study was conducted at concentrations ranging from 1/2 to 2 MIC for each isolate. The concentration of drug formulations compared to free meropenem MIC was calculated for physical composition, and the results are reported as biofilm growth inhibition percentage (BGI%) (Fig. 4).

3.6. Biofilm gene expression analysis

The ½ concentrations of niosome-encapsulated meropenem and free meropenem were used to examine the expression of the biofilm genes *icaD, FnbA, Ebps*, and *Bap* using quantitative Real-Time PCR. According to the results, the highest decline in the expression of *icaD, FnbA, Ebps*, and *Bap* was observed after treatment with niosome-encapsulated meropenem ($p < 0.05$) (Fig. 5A and B). Among the various formulations, F1 significantly reduced the expression of biofilm genes compared with the other formulations. Among various formulations, F1 Among the various formulations, F1 significantly reduced the expression of biofilm genes compared to other formulations significantly reduced the expression of biofilm genes compared to other formulations and free meropenem.

3.7. Cytotoxicity

The cytotoxicity of various niosomal formulations was compared with that of free meropenem in the HDF normal cell line. Niosome-encapsulated meropenem exhibited negligible cytotoxicity compared with free meropenem at all tested concentrations. Almost, 68.35 ± 1.28 of the cells survived for 24 h after treatment with 256 µg/ml meropenem while over 90.27 ± 2.41 % of the cells survived for 24 h after incubation with the F1 formulation of niosome-encapsulated meropenem. In addition, cell viability was 75.21 ± 1.32 %, 86.24 ± 2.32 %, and 79.65 ± 3.54 %, for the formulations of F2, F3, and F4, respectively at 256 µg/ml (Fig. 6).

4. Discussion

Methicillin-resistant Staphylococcus aureus (MRSA) is a prevalent hospital pathogen that has increased worldwide over the past three decades and poses a serious threat to nosocomial infection [31]. MRSA strains are resistant to various antimicrobial agents, including vancomycin [32]. The current study assessed the sensitivity of different isolates and found that 40 isolates (24.69 %)
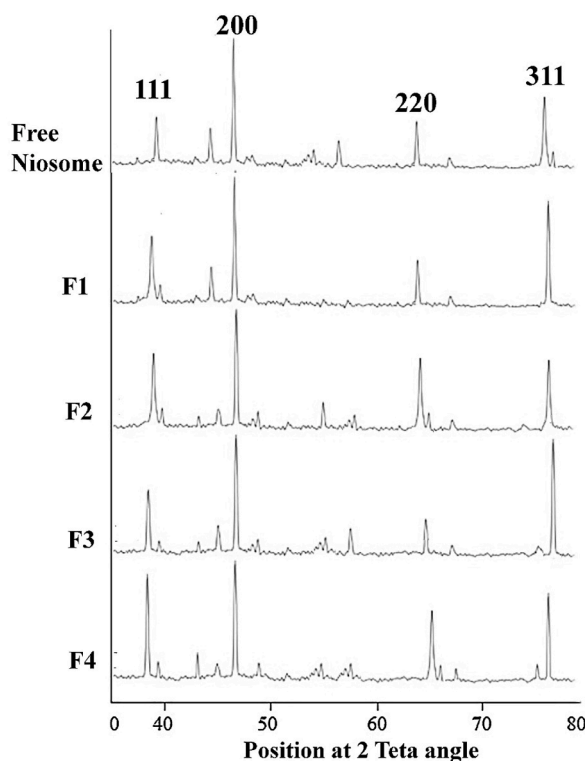
Fig. 2. The XRD pattern of niosome-encapsulated meropenem formulations.

methicillin-resistant *S. aureus* (MRSA). Moreover, 72.38 % of the isolates formed biofilms, which are among the main factors of AMR. Biofilm development in MRSA strains slows the penetration of antimicrobial agents and complicates the treatment of infections caused by these bacteria [33]. As a result, new treatment options and techniques for minimizing MRSA resistance are critical. The present study investigated the ability of niosome-encapsulated meropenem to enhance antimicrobial activity against MRSA [34]. Non-ionic surfactants including Tween 60, Tween 40, and as well as Span 60 and Span 40 combined with cholesterol, were used to create a variety of niosomal formulations. Because different cholesterol levels may cause different bilayers in the formulations and affect their bilayer surface load, the cholesterol content was kept constant throughout the formulations. As a consequence, by maintaining cholesterol consistency throughout all formulations, the niosome membrane's strength and resistance to ultrasonic waves were maintained, resulting in more consistent vesicles in terms of size [35]. Various surfactant combinations, on the other hand, lead to nanostructures with a variety of morphological characteristics [36]. Different results were obtained when the Tween and Span ratios were equal. Because of its high hydrophilicity, Tween 60 reduces the strength of niosome membranes [37]. This flaw was fixed by mixing equal amounts of the Span 60 surfactant [50:50], which is more hydrophobic and results in dense niosome films. Tween 60 and Span 60, on the other hand, had greater phase transfer temperatures than the other surfactants studied, resulting in enhanced drug encapsulation [38]. The long-saturated alkyl chain of Span 60 resulted in more preamble niosome, resulting in greater drug encapsulation [39]. Furthermore, the lipophilic balance of the Span 60 surfactant was 4.7, which was lower than that of Span 40 [6.7], resulting in the formation of smaller vesicles [40,41]. In comparison with the other formulations, the F1 formulation was shown to have better acceptable size and morphological properties. Due to their strong hydrophilic-lipophilic balance, the Span 40 used in the F2, F3, and F4 formulations resulted in larger vesicles than those in F1. Due to the unsaturated alkyl chains in Span 40, F2, F3, and F4 formulations had fewer encapsulated meropenem despite their larger size, resulting in decreased Encapsulation Efficiency (EE%). As a result, the size achieved for the F1 formulation was much smaller than that of the other three formulations, indicating a greater EE for this formulation. The most stable niosome-encapsulated meropenem was found in formulation F1, which exhibited a zeta potential of -65.29 ± 2.68 across 56 days at 4 °C and 25 °C. Additionally, drug stability was higher at 4 °C than at 25 °C, which might be due to lower niosome bilayer mobility at 4 °C [42]. Furthermore, an earlier study found that negative zeta potentials result from electrostatic repulsion between particles, which increases niosome stability [43]. Given the niosome bilayer structure, the drug might reside either in the center of the niosome within the two layers or at the surface of the niosome during encapsulation [44]. Therefore, the drugs on the surface begin to be released over the first hours, resulting in the blast phase (fast drug release). After 7 h, surface drugs are released, and encapsulated drugs residing at the center of the niosome and on the bilayer membrane start to be released, resulting in a controlled drug release and a stable phase. On the other hand, the cholesterol present in the system stops gel-to-lipid phase transfer in niosome systems, which prevents the drug from leaking out of the niosome, resulting in controlled drug release over the long term and efficient drug release [45].
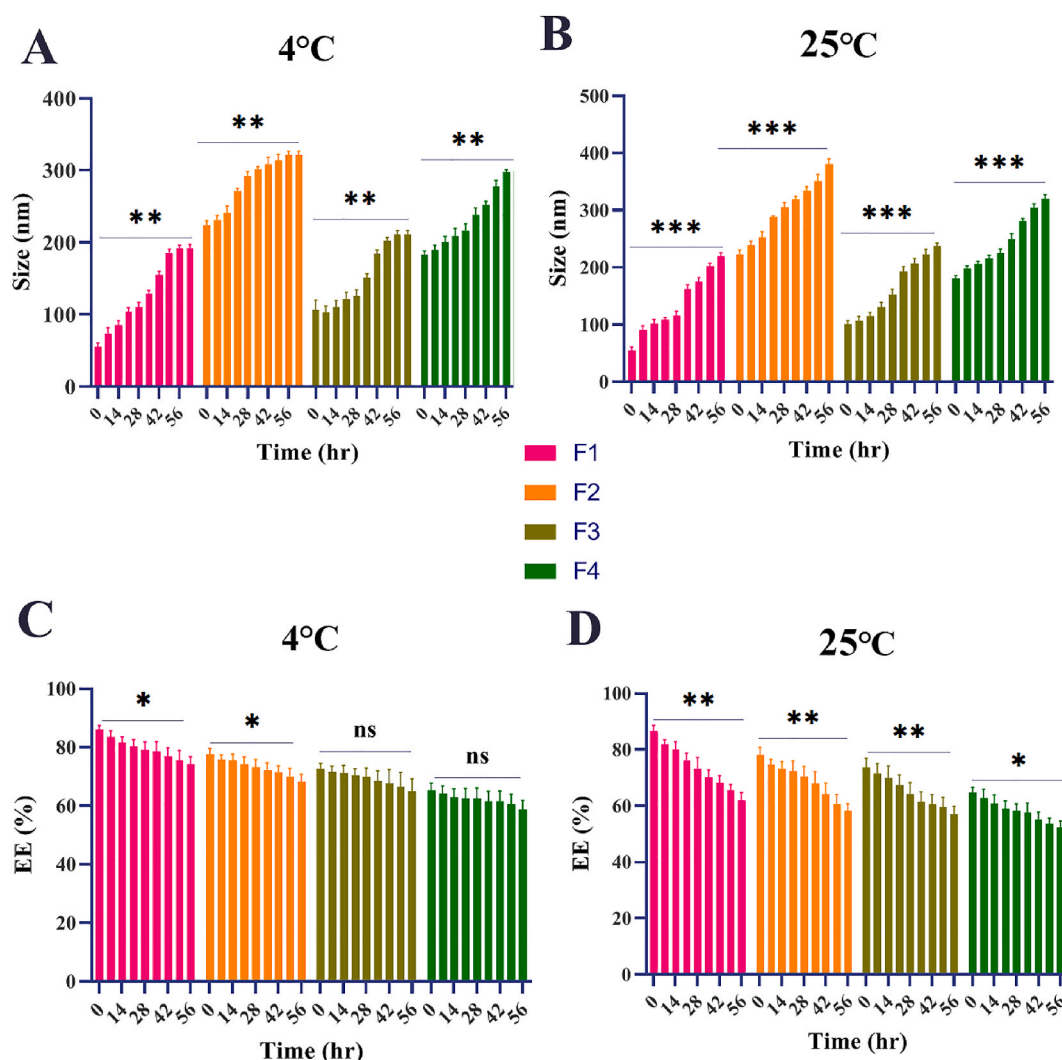
Fig. 3. Impact of temperature and shelf time on the average size at 4 °C (A) and 25 °C (B) and encapsulation efficiency at 4 °C (C) and 25 °C (D) of the niosome-encapsulated meropenem.

Table 4
Antibiotic susceptibility profile of *S. aureus* isolates and biofilm gene distribution.

Strain NO.	Resistance pattern	Biofilm gene			
		icaD	FnbA	Ebps	Bap
$S_{MRSA}1$	VA, FOX, CD, MUP, MEM	+	+	+	+
$S_{MRSA}2$	VA, FOX, CIP, CD,MUP, MEM	+	+	+	+
$S_{MRSA}3$	VA, FOX, CD, MUP, MEM	+	+	+	+
$S_{MRSA}4$	VA, FOX,CIP, CD, MUP, MEM	+	+	+	+
$S_{MRSA}5$	VA, FOX, CIP, CD,MUP,MEM	+	+	+	+
$S_{MRSA}6$	VA, FOX, CD, MUP, MEM	+	+	+	+

FOX: Cefoxitin, VA: Vancomycin, CD: Clindamycin, MU: Mupirocin, CIP: Ciprofloxacin, MEM: Meropenem.

Formulation F1 creates stronger connections with cholesterol because of its increased strength and superior surface density, resulting in faster medication delivery. Fig. 3 shows that this formulation has the longest feasible regulated medication release time feasible (312 h). Hedayati et al. prepared various niosome-encapsulated tobramycin formulations based on Span 60 and Tween 60, reporting that the sizes of the niosome-encapsulated tobramycin varied among the different formulations. The niosomal formulations prepared in this study had an EE% of 69.54 % ±; 0.67, so they had high stability in 60 days with a very small reduction in size and EE%, indicating that they are suitable candidates for pharmaceutical applications. Mansouri et al. synthesized niosomes containing

Table 5
MIC, MBC, and MBIC values of free meropenem and various niosome-encapsulated meropenem formulations against MRSA strains.

S. aureus isolates	Biofilm Phenotype	MRSA	MDR	Free meropenem			Niosome encapsulated meropenem			
				MIC (µg/ml)	MBC (µg/ml)	MBIC (µg/ml)	Formulation	MIC (µg/ml)	MBC (µg/ml)	MBIC (µg/ml)
S_{MRSA}1	Strong	+	+	4	8	2	F1	0.25	0.50	0.125
							F2	1.0	2.0	0.50
							F3	0.5	1.0	0.25
							F4	1.0	1.0	0.50
S_{MRSA}2	Strong	+	+	4	4	2	F1	0.125	0.25	0.062
							F2	0.50	1.0	0.25
							F3	0.125	0.25	0.125
							F4	0.25	0.50	0.125
S_{MRSA}3	Strong	+	+	8	16	4	F1	0.25	0.50	0.125
							F2	2.0	4	1.0
							F3	0.50	1.0	025
							F4	1.0	2.0	0.50
S_{MRSA}4	Strong	+	+	2	4	2	F1	0.125	0.25	0.125
							F2	1.0	1.0	0.50
							F3	0.25	0.50	0.125
							F4	0.50	1.0	0.25
S_{MRSA}5	Strong	+	+	8	8	4	F1	0.50	1.0	0.25
							F2	2.0	4.0	1.0
							F3	1.0	2.0	0.50
							F4	1.0	2.0	1.0
S_{MRSA}6	Strong	+	+	4	8	4	F1	0.125	0.25	0.062
							F2	2.0	2.0	1.0
							F3	0.25	0.50	0.125
							F4	0.50	1.0	0.25
ATCC 33592	Moderate	+	+	2	4	2	F1	0.125	0.25	0.125
							F2	1.0	2.0	0.50
							F3	0.125	0.25	0.062
							F4	0.50	1.0	0.25

streptomycin sulfate using the thin-layer hydration method and optimized the niosomes based on their size, polydispersity index (PDI), and encapsulation efficiency (EE%). The results of this study showed that the ratio of Span 60 to Tween 60 was 1.5, and the ratio of surfactant to cholesterol was 1.02, leading to the optimal formulation with minimum size, low PDI, and maximum EE% of 97.8 nm, 0.27, and 86.7 %, respectively. In addition, Mirzaie et al. studied the preparation and optimization of ciprofloxacin-encapsulated niosomes. In this study, the formulation of niosome-encapsulated ciprofloxacin was optimized by changing the proportions of Tween 60, Span 60, and cholesterol. The prepared niosomal formulations exhibited high storage stability for up to 30 days with little change in size or drug entrapment efficiency during storage. The present study improved the antibacterial activity of niosome-encapsulated meropenem. Hence, antibacterial assays were conducted after isolation and determination of the MRSA strains. The MIC of niosome -encapsulated meropenem 's MIC was much lower than that of free meropenem, indicating the drug's increased efficiency of the drug's antibacterial activity. Heba et al. suggested that loading vancomycin into niosomes improves their anti-biofilm and antibacterial activity against *S. aureus* isolates [46,47]. Numerous studies have reported the potential of niosomes to increase antibiotic activity through targeted drug delivery and protect antibiotics from unfavorable environmental conditions [48,49]. According to Phikunthong et al. niosomes have great potential for encapsulating nisin and improving its antibacterial activity [50,51]. According to Tinnakorn et al. cholesterol in niosome increases targeted drug delivery to bacteria by attaching it to the lipid membrane of the bacteria [52]. Consistent with Zafari's findings, our results showed increased antibacterial activity in niosome-encapsulated antibiotics [53,54]. According to Gupta et al. there are various absorption and fusion mechanisms between the niosome and the bacterial wall that could result in increased targeted drug delivery [55,56].

The other aim of the present study was to examine the anti-biofilm properties of niosome-encapsulated meropenem and free meropenem in the form of biofilm formation inhibition, biofilm growth inhibition, and reduction of biofilm-involved gene expression. The MBIC of niosome -encapsulated meropenem MBIC was four to six times lower than that of free meropenem in all of the studied isolates, indicating the higher efficiency of niosome compared to free meropenem. On the other hand, the F1 niosome-encapsulated meropenem formulation exhibited the highest biofilm and growth inhibition. Therefore, one of the study objectives was to investigate the anti-biofilm activity of niosome -encapsulated and free meropenem. After 2 h of treatment with drugs for 24 h, biofilm growth and maturation inhibition were observed using MIC, 1/2 MIC, and 2MIC concentrations of various formulations of niosome-encapsulated meropenem and free meropenem. The best biofilm growth inhibition performance was observed in Formulation F1 of niosome-encapsulated meropenem, demonstrating that the encapsulation of antibiotics has an influence on their enhanced efficiency and biofilm development inhibition, which is consistent with Barakat et al. In the present study, we examined the impact of niosome-encapsulated meropenem at each sub-MIC concentration on *icaD, FnbA, Ebps*, and *Bap* biofilm gene expression. The results revealed a significant decrease in the expression of these genes compared to free meropenem. Furthermore, the F1 formulation had the most significant impact on reducing gene expression and was thus determined to be the optimal formulation. Reduced expression of the
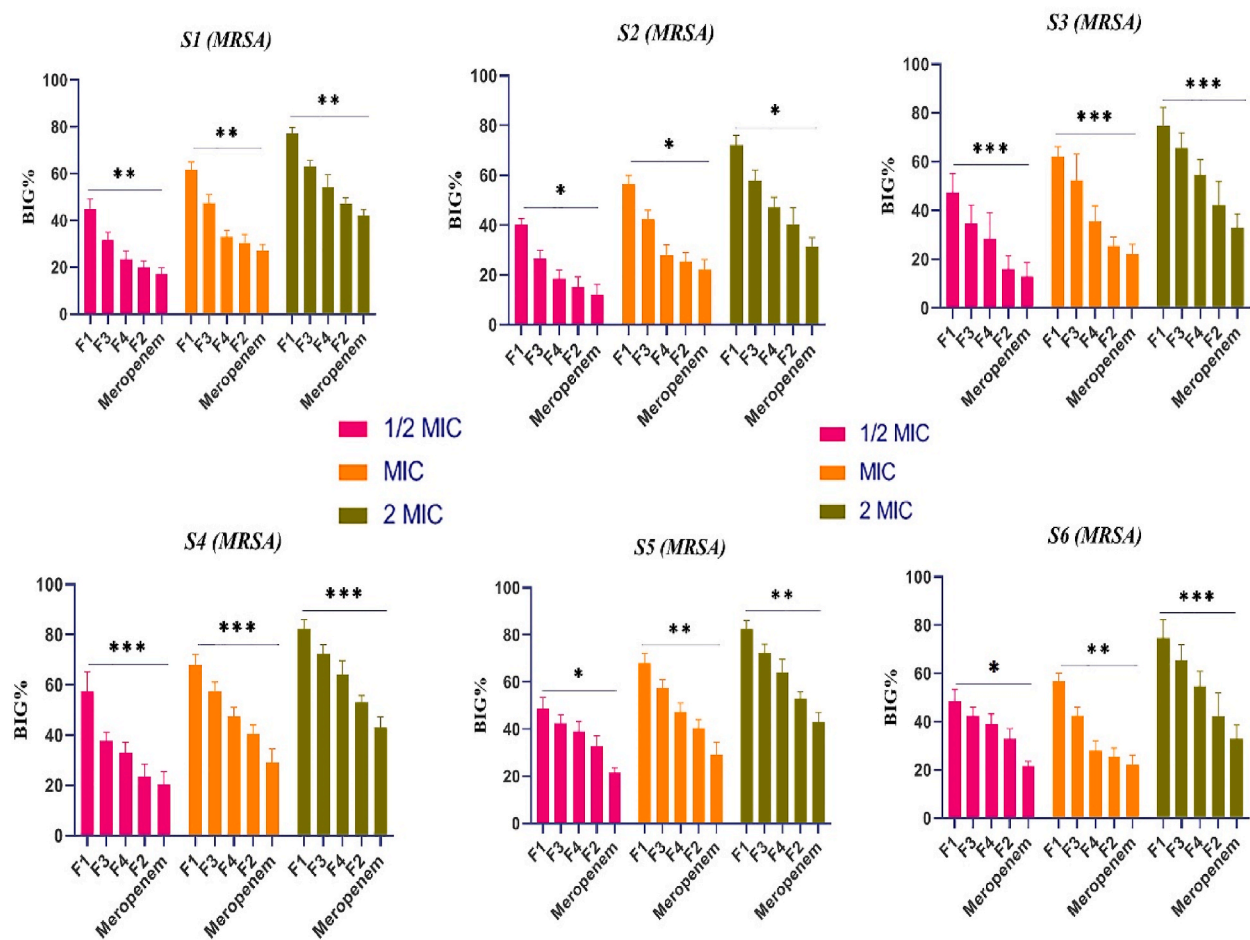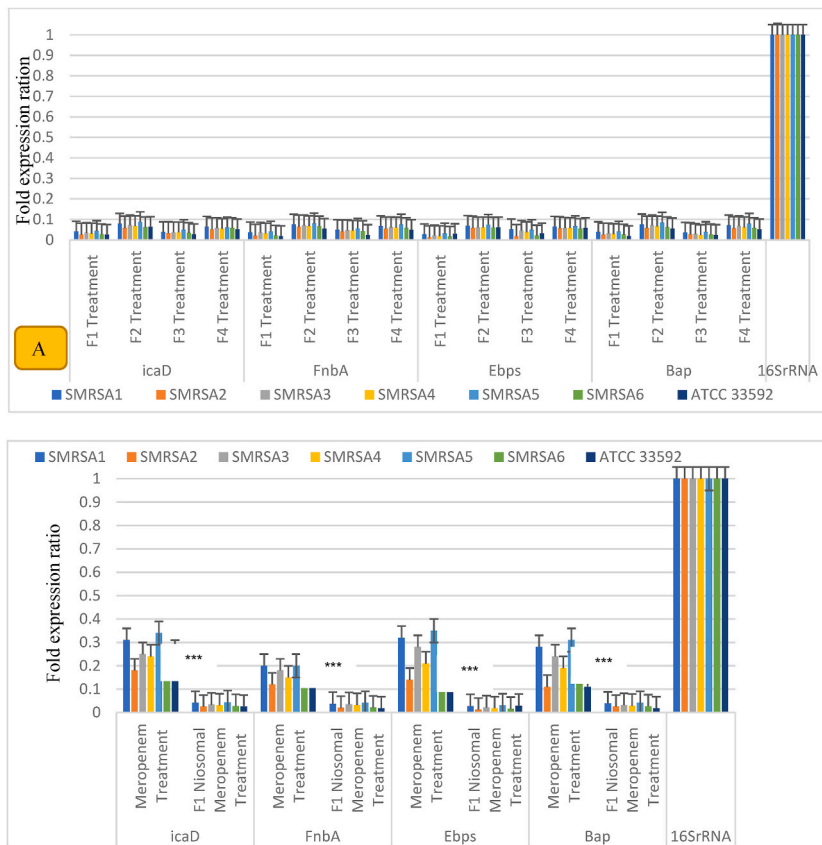
Fig. 4. Biofilm growth inhibition percentage (BGI%) of various formulations of niosome-encapsulated meropenem. Data are mean ± SD of three independent experiments. The significance level was determined as ***p < 0.0001, **p < 0.01, *p < 0.00.5.

mentioned genes could potentially lead to an interaction between niosome-encapsulated meropenem and transcription factors, ultimately resulting in transcription inhibition or decrease [57–63]. These findings are consistent with those of Lawson et al. who found that nano-encapsulation influenced the enhancement of biofilm inhibition and reduction of biofilm gene expression [64]. According to Abdelaziz et al. norfloxacin encapsulation in niosomes increases the anti-biofilm characteristics in multidrug-resistant (MDR) bacteria [65].

The finding of novel antibacterial chemicals that are non-toxic to mammalian cells has attracted the attention of pharmaceutical researchers [64,66–69]. The toxicity of niosome-encapsulated meropenem formulations on HDF cells was investigated using the conventional MTT technique, which revealed that groups treated with niosome-encapsulated meropenem had a higher cell viability rate than those treated with free meropenem. In comparison to other formulations, formulation F1 of niosome-encapsulated meropenem showed the lowest cytotoxicity, with cell survival of over 90 % after 24 h.

5. Conclusion

Niosome-encapsulated meropenem is a new approach for restoring meropenem characteristics at a low cost, giving meropenem distinct new properties such as increased targeted drug delivery, maintaining stability, and controlling drug release. According to this study, this niosomal formulation of meropenem is more effective than free meropenem against methicillin-resistant *Staphylococcus aureus* (MRSA) isolates that are resistant to a variety of antibiotics, especially vancomycin and methicillin, and the present study is the first to report the impacts of encapsulating meropenem in the niosome on biofilm formation and growth inhibition and biofilm eradication against MRSA clinical isolates. According to the present study results, it could be inferred that niosome encapsulation of meropenem increases its antibacterial and anti-biofilm activities against MRSA strains, and these formulations could be considered a new strategy for targeted drug delivery.

Fig. 5. A: Effect of various niosomal formulations on biofilm gene expression. B: effect of the optimum niosome formulation (F1) on biofilm gene expression compared with free meropenem. Data are mean ± SD of three independent experiments. The significance level was determined as ***$p < 0.0001$.
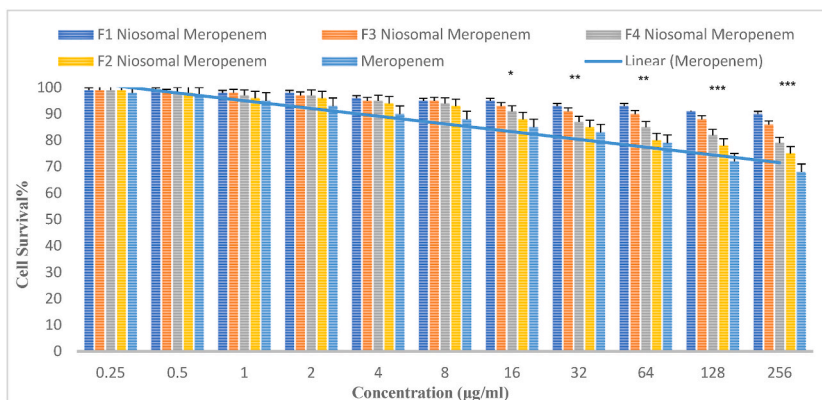
Fig. 6. Cell viability percentage of HDF cells treated with various formulations of niosome-encapsulated meropenem in comparison with free niosome over 24 h. Data are mean ± SD of three independent experiments. The significance level was determined as ***$p < 0.0001$, **$p < 0.01$, *$p < 0.00.5$.

Ethics declarations

Ethics approval and consent to participate

Written informed consent for publication of their details was obtained from the study participant. All protocols were performed by the Ethical Committee and Research Deputy of the Islamic Azad University of Shahrekord Branch, Iran for the Care and Use of

Laboratory Animals, and were approved by the Institutional Care and Use Committee guidelines of Islamic Azad University, Shahrekord, Iran (14th 2020 with ethics code: IR.IAU.SHK.REC.1400.043).

Consent for publication

Not applicable.

Availability of data

Data will be available on request.

Funding

There is no funding source.

CRediT authorship contribution statement

Kamal Paseban: Investigation. **Sama Noroozi:** Methodology. **Rokhshad Gharehcheloo:** Data curation. **Abbas Haddadian:** Investigation. **Farnoush Falahi Robattorki:** Methodology. **Hedieh Dibah:** Validation. **Reza Amani:** Software. **Fatima Sabouri:** Investigation. **Erfan Ghanbarzadeh:** Data curation. **Shadi Hajrasouiha:** Writing – original draft. **Arezou Azari:** Formal analysis. **Tina Rashidian:** Investigation. **Amir Mirzaie:** Conceptualization. **Zahra Pirdolat:** Methodology. **Massoumeh Salarkia:** Formal analysis. **Dorsa Sadat Shahrava:** Data curation. **Fatemeh Safaeinikjoo:** Methodology. **Atena Seifi:** Methodology. **Niusha Sadat Hosseini:** Investigation. **Niloofar Saeinia:** Methodology. **Aliasghar Bagheri Kashtali:** Investigation. **Ali Ahmadiyan:** Methodology. **Roza Mazid Abadi:** Investigation. **Faezeh Sadat Kermani:** Writing – review & editing. **Romina Andalibi:** Formal analysis. **Arman Chitgarzadeh:** Investigation. **Aryan Aryan Tavana:** Formal analysis. **Tohid Piri Gharaghie:** Investigation.

Declaration of competing interest

The authors declare the following financial interests/personal relationships which may be considered as potential competing interests:Amir Mirzaie reports administrative support was provided by Islamic Azad University.Amir Mirzaie reports a relationship with Islamic Azad University that includes: employment. Amir Mirzaie has patent pending to assignee. There is no conflict of interest. If there are other authors, they declare that they have no known competing financial interests or personal relationships that could have appeared to influence the work reported in this paper.

Acknowledgments

Appendix A. Supplementary data

Supplementary data to this article can be found online at https://doi.org/10.1016/j.heliyon.2024.e35651.

References

[1] Shamshul Ansari, et al., Recent advances in *Staphylococcus aureus* infection: focus on vaccine development, Infect. Drug Resist. 12 (2019) 1243.
[2] Carmen González, et al., Bacteremic pneumonia due to *Staphylococcus aureus*: a comparison of disease caused by methicillin-resistant and methicillin-susceptible organisms, Clin. Infect. Dis. 29 (5) (1999) 1171–1177.
[3] Nicholas A. Turner, et al., Methicillin-resistant *Staphylococcus aureus*: an overview of basic and clinical research, Nat. Rev. Microbiol. 17 (4) (2019) 203–218.
[4] Yunlei Guo, et al., Prevalence and therapies of antibiotic-resistance in *Staphylococcus aureus*, Front. Cell. Infect. Microbiol. 10 (2020) 107.
[5] Douglas N. Fish, Meropenem in the treatment of complicated skin and soft tissue infections, Therapeut. Clin. Risk Manag. 2 (4) (2006) 401.
[6] U. Liebchen, et al., Therapeutic drug monitoring-guided high dose meropenem therapy of a multidrug resistant Acinetobacter baumannii-A case report, Respiratory Medicine Case Reports 29 (2020) 100966.
[7] Patrick R. Gonzales, et al., Synergistic, collaterally sensitive β-lactam combinations suppress resistance in MRSA, Nat. Chem. Biol. 11 (11) (2015) 855–861.
[8] Ann A. Elshamy, Khaled M. Aboshanab, A review on bacterial resistance to car*Bap*enems: epidemiology, detection and treatment options, Future Science OA 6 (3) (2020) FSO438.
[9] Bart N. Green, et al., Methicillin-resistant *Staphylococcus aureus*: an overview for manual therapists, Journal of Chiropractic Medicine 11 (1) (2012) 64–76.
[10] Zohra Khatoon, et al., Bacterial biofilm formation on implantable devices and approaches to its treatment and prevention, Heliyon 4 (12) (2018) e01067.
[11] Gebreselema Gebreyohannes, et al., Challenges of intervention, treatment, and antibiotic resistance of biofilm-forming microorganisms, Heliyon 5 (8) (2019) e02192.
[12] Christophe Beloin, Jean-Marc Ghigo, Finding gene-expression patterns in bacterial biofilms, Trends Microbiol. 13 (1) (2005) 16–19.

[13] Mostafa Nemati, et al., Screening of genes encoding adhesion factors and biofilm formation in *Staphylococcus aureus* isolates from poultry, Avian Pathol. 38 (6) (2009) 513–517.

[14] T.J. Foster, The remarkably multifunctional fibronectin binding proteins of *Staphylococcus aureus*, Eur. J. Clin. Microbiol. Infect. Dis. 35 (12) (2016) 1923–1931.

[15] Pietro Speziale, Giampiero Pietrocola, The multivalent role of fibronectin-binding proteins A and B (FnBPA and FnBPB) of *Staphylococcus aureus* in host infections, Front. Microbiol. 11 (2020) 2054.

[16] Barbara Kot, Hubert Sytykiewicz, Iwona Sprawka, Expression of the biofilm-associated genes in methicillin-resistant *Staphylococcus aureus* in biofilm and planktonic conditions, Int. J. Mol. Sci. 19 (11) (2018) 3487.

[17] Piri Gharaghie, Tohid, Seyed Ataollah Sadat Shandiz, "The inhibitory effects of silver nanoparticles on *Bap* gene expression in antibiotic-resistant acientobacter bumanni isolates using real-time PCR.", Scientific Journal of Ilam University of Medical Sciences 26 (4) (2018) 175–185.

[18] R. Vazquez-Muñoz, et al., Enhancement of antibiotics antimicrobial activity due to the silver nanoparticles impact on the cell membrane, PLoS One 14 (11) (2019) e0224904.

[19] Ángela Martin-Serrano, et al., Nanosystems as vehicles for the delivery of antimicrobial peptides (AMPs), Pharmaceutics 11 (9) (2019) 448.

[20] Raquel Becerril, Cristina Nerín, Filomena Silva, Encapsulation systems for antimicrobial food packaging components: an update, Molecules 25 (5) (2020) 1134.

[21] Xuemei Ge, et al., Advances of non-ionic surfactant vesicles (niosomes) and their application in drug delivery, Pharmaceutics 11 (2) (2019) 55.

[22] Pei Ling Yeo, et al., Niosomes: a review of their structure, properties, methods of preparation, and medical applications, Asian Biomed. 11 (4) (2018) 301–314.

[23] Saliha Durak, et al., Niosomal drug delivery systems for ocular disease—recent advances and future prospects, Nanomaterials 10 (6) (2020) 1191.

[24] H.K. Tiwari, M.R. Sen, Emergence of vancomycin resistant *Staphylococcus aureus* (VRSA) from a tertiary care hospital from northern part of India, BMC Infect. Dis. 6 (2006) 156.

[25] Ying-Qi Xu, et al., Niosome encapsulation of curcumin: characterization and cytotoxic effect on ovarian cancer cells, J. Nanomater. 2016 (2016).

[26] Ghada Abdelbary, Nashwa El-gendy, Niosome-encapsulated gentamicin for ophthalmic controlled delivery, AAPS PharmSciTech 9 (3) (2008) 740–747.

[27] S.P. Vyas, V. Sihorkar, S. Jain, Mannosylated liposomes for bio-film targeting, Int. J. Pharm. 330 (1–2) (2007) 6–13.

[28] Laura Cianfruglia, et al., Side effects of curcumin: epigenetic and antiproliferative implications for normal dermal fibroblast and breast cancer cells, Antioxidants 8 (9) (2019) 382.

[29] Terry L. Riss, et al., Cell viability assays assay guidance manual. Assay Guidance Manual, 2004, pp. 1–23.

[30] Weijia Li, Jing Zhou, Yuyin Xu, Study of the in vitro cytotoxicity testing of medical devices, Biomedical reports 3 (5) (2015) 617–620.

[31] CJ Ghia, S Waghela, G Rambhad, A systemic literature review and meta-analysis reporting the prevalence and impact of methicillin-resistant *Staphylococcus aureus* infection in India, Infect. Dis. (Auckl) 13 (2020), 1178633720970569.

[32] Fateh Rahimi, et al., Antibiotic resistance pattern of methicillin resistant and methicillin sensitive *Staphylococcus aureus* isolates in Tehran, Iran, Jundishapur J. Microbiol. (2013) 144–149.

[33] Marie Ebob Agbortabot Bissong, Collins Njie Ateba, Genotypic and phenotypic evaluation of biofilm production and antimicrobial resistance in *Staphylococcus aureus* isolated from milk, north west province, South Africa, Antibiotics 9 (4) (2020) 156.

[34] Rita Muzzalupo, Lorena Tavano, Niosomal drug delivery for transdermal targeting: recent advances, Res. Rep. Transdermal Drug Deliv. 4 (2015) 23.

[35] S. Sadeghi, H. Bakhshandeh, R. Ahangari Cohan, A. Peirovi, P. Ehsani, D. Norouzian, Synergistic anti-staphylococcal activity of niosomal recombinant lysostaphin-LL-37, Int. J. Nanomed. 14 (2019) 9779792.

[36] Wenbo Wei, Feng Bai, Hongyou Fan, Surfactant-assisted cooperative self-assembly of nanoparticles into active nanostructures, iScience 11 (2019) 272–293.

[37] E. Moazeni, K. Gilani, F. Sotoudegan, et al., Formulation and in vitro evaluation of ciprofloxacin containing niosomes for pulmonary delivery, J. Microencapsul. 27 (2010) 618–627.

[38] Vajihe Akbari, et al., Release studies on ciprofloxacin loaded non-ionic surfactant vesicles, Avicenna J. Med. Biotechnol. (AJMB) 7 (2) (2015) 69.

[39] Y. Hao, F. Zhao, N. Li, Y. Yang, K. Li, Studies on a high encapsulation of colchicine by a niosome system, Int. J. Pharm. 244 (1–2) (2002) 73–80.

[40] Diana E. Aziz, Ahmed Abdelbary Aly, Abdelhalim Ibrahim Elassasy, Implementing central composite design for developing transdermal diacerein-loaded niosomes: ex vivo permeation and in vivo deposition, Curr. Drug Deliv. 15 (9) (2018) 1330–1342.

[41] Ch Hedayati, Mojtaba, et al., "Niosome-encapsulated tobramycin reduced antibiotic resistance and enhanced antibacterial activity against multidrug-resistant clinical strains of Pseudomonas aeruginosa.", J. Biomed. Mater. Res. (2020).

[42] M. Khaleghian, H. Sahrayi, Y. Hafezi, M. Mirshafeeyan, Z.S. Moghaddam, In silico design and mechanistic study of niosome-encapsulated curcumin against multidrug-resistant Staphylococcus aureus biofilms, Front. Microbiol. 14 (2023) 1277533.

[43] H.S. Barakat, M.A. Kassem, L.K. El-Khordagui, N.M. Khalafallah, Vancomycin-eluting niosomes: a new approach to the inhibition of staphylococcal biofilm on abiotic surfaces, AAPS PharmSciTech 15 (5) (2014) 1263–1274.

[44] Karim Masud Kazi, et al., Niosome: a future of targeted drug delivery systems, \"J. Adv. Pharm. Technol. Research\"\" (JAPTR)\" 1 (4) (2010) 374.

[45] A. Balasubramaniam, V.A. Kumar, K.S. Pillai, Formulation and in vivo evaluation of niosome-encapsulated daunorubicin hydrochloride, Drug Dev. Ind. Pharm. 28 (2002) 1181–1193.

[46] R.M. Derbali, V. Aoun, G. Moussa, et al., Tailored nanocarriers for the pulmonary delivery of levofloxacin against *Pseudomonas aeruginosa*: a comparative study, Mol. Pharm. 16 (5) (2019) 1906–1916.

[47] Heba S. Barakat, et al., Vancomycin-eluting niosomes: a new approach to the inhibition of staphylococcal biofilm on abiotic surfaces, AAPS PharmSciTech 15 (5) (2014) 1263–1274.

[48] Linlin Wang, Chen Hu, Longquan Shao, The antimicrobial activity of nanoparticles: present situation and prospects for the future, Int. J. Nanomed. 12 (2017) 1227.

[49] Lukas Gritsch, "An investigation on antibiotic-free antibacterial materials combining bioresorbable polyesters, chitosan and therapeutic ions." (2019).

[50] Phikunthong Kopermsub, Varissaporn Mayen, Choochart Warin, Potential use of niosomes for encapsulation of nisin and EDTA and their antibacterial activity enhancement, Food Res. Int. 44 (2) (2011) 605–612.

[51] Theansungnoen, Tinnakorn, et al. "FORMULATION AND EVALUATION OF NIOSOMES ENCAPSULATED WITH KT2 AND RT2: ANTIMICROBIAL AND ANTICANCER PEPTIDES DERIVED FROM CROCODILE LEUKOCYTE EXTRACT.".

[52] Rashed N. Al, R.M. Joji, N.K. Saeed, K.M. Bindayna, Detection of overexpression of efflux pump expression in fluoroquinolone-resistant Pseudomonas aeruginosa isolates, Int J Appl Basic Med Res. 10 (2020) 37–42.

[53] Vajihe Akbari, et al., Ciprofloxacin nano-niosomes for targeting intracellular infections: an in vitro evaluation, J. Nanoparticle Res. 15 (4) (2013) 1556.

[54] Noelia D. Machado, et al., Niosomes encapsulated in biohydrogels for tunable delivery of phytoalexin resveratrol, RSC Adv. 9 (14) (2019) 7601–7609.

[55] P.V. Gupta, A.M. Nirwane, M.S. Nagarsenker, Inhalable levofloxacin liposomes complemented with lysozyme for treatment of pulmonary infection in rats: effective antimicrobial and antibiofilm strategy, AAPS PharmSciTech 19 (2018) 1454–1467.

[56] S. Manandhar, A. Singh, A. Varma, S. Pandey, N. Shrivastava, Evaluation of methods to detect in vitro biofilm formation by staphylococcal clinical isolates, BMC Res. Notes 11 (1) (2018) 714.

[57] A. Ikonomidis, A. Vasdeki, I. Kristo, A.N. Maniatis, A. Tsakris, K.N. Malizos, S. Pournaras, Association of biofilm formation and methicillin resistance with accessory gene regulator (agr) loci in Greek *Staphylococcus aureus* clones, Microb. Pathog. 47 (6) (2009 Dec) 341–344.

[58] S. Manandhar, A. Singh, A. Varma, S. Pandey, N. Shrivastava, Biofilm producing clinical *Staphylococcus aureus* isolates augmented prevalence of antibiotic resistant cases in tertiary care hospitals of Nepal, Front. Microbiol. 9 (2018) 2749.

[59] Debjani Banerjee, et al., A review on basic biology of bacterial biofilm infections and their treatments by nanotechnology-based approaches, Proc. Natl. Acad. Sci. India B Biol. Sci. (2019) 1–17.

[60] Gedif Meseret Abebe, The role of bacterial biofilm in antibiotic resistance and food contamination, International Journal of Microbiology (2020).

[61] Heba S. Barakat, Mervat A. Kassem, Vancomycin-Eluting niosomes: a new approach to the inhibition of staphylococcal biofilm on abiotic surfaces, AAPS PharmSciTech 15 (2014).

[62] C. Cucarella, M.A. Tormo, E. Knecht, B. Amorena, I. Lasa, T.J. Foster, J.R. Penadés, Expression of the biofilm-associated protein interferes with host protein receptors of *Staphylococcus aureus* and alters the infective process, Infect. Immun. 70 (6) (2002) 3180–3186.

[63] S. Manandhar, A. Singh, A. Varma, S. Pandey, N. Shrivastava, Evaluation of methods to detect in vitro biofilm formation by staphylococcal clinical isolates, BMC Res. Notes 11 (1) (2018) 714.

[64] M. Lawson, K. Hoth, C. DeForest, C. Bowman, K. Anseth, Inhibition of *Staphylococcus epidermidis* biofilms using polymerizable vancomycin derivatives, Clin. Orthop. Relat. Res. 468 (8) (2010) 2081–2091.

[65] A.A. Abdelaziz, T.E. Elbanna, F.I. Sonbol, N.M. Gamaleldin, G.M. El Maghraby, Optimization of niosomes for enhanced antibacterial activity and reduced bacterial resistance: in vitro and in vivo evaluation, Expet Opin. Drug Deliv. 12 (2) (2015) 163–180.

[66] H.-J. Kim, Gias EL. Michael, M.N. Jones, The adsorption of cationic liposomes to *Staphylococcus aureus* biofilms, Colloids Surf A Physicochem Eng Aspects 149 (1–3) (1999) 561–570.

[67] Yajie Zhong, et al., Natural polymer-based antimicrobial hydrogels without synthetic antibiotics as wound dressings, Biomacromolecules 21 (8) (2020) 2983–3006.

[68] D. Poy, A. Akbarzadeh, Shahmabadi H. Ebrahimi, et al., Preparation, characterization, and cytotoxic effects of liposomal nanoparticles containing cisplatin: an in vitro study, Chem. Biol. Drug Des. 88 (2016) 568–573.

[69] Laxmi Gayatri Sorokhaibam, M. Ahmaruzzaman, Phenolic Wastewater Treatment: Development and Applications of New Adsorbent Materials, Butterworth-Heinemann, Oxford, England, 2014.